

RSC Advances



This is an *Accepted Manuscript*, which has been through the Royal Society of Chemistry peer review process and has been accepted for publication.

Accepted Manuscripts are published online shortly after acceptance, before technical editing, formatting and proof reading. Using this free service, authors can make their results available to the community, in citable form, before we publish the edited article. This *Accepted Manuscript* will be replaced by the edited, formatted and paginated article as soon as this is available.

You can find more information about *Accepted Manuscripts* in the [Information for Authors](#).

Please note that technical editing may introduce minor changes to the text and/or graphics, which may alter content. The journal's standard [Terms & Conditions](#) and the [Ethical guidelines](#) still apply. In no event shall the Royal Society of Chemistry be held responsible for any errors or omissions in this *Accepted Manuscript* or any consequences arising from the use of any information it contains.



Journal Name

ARTICLE

Received 00th January 20xx,
Accepted 00th January 20xx

DOI: 10.1039/x0xx00000x

www.rsc.org/

Design and Preparation of Non-enzymatic Hydrogen Peroxide Sensor based on a Novel Rigid Chain Liquid Crystalline Polymer/Reduced Graphene Oxide Composite

Ya-qi Yang, He-lou Xie*, Jun Tang, Shuai Tang, Jie Yi*, Hai-liang Zhang*

ABSTRACT: A novel non-enzymatic hydrogen peroxide (H_2O_2) sensor was developed using rigid chain liquid crystalline (LC) polymer and reduced graphene oxide (rGO) composite. Firstly, we synthesized a novel rigid chain LC polymer with ferrocenyl as the side group. The chemical structures of the monomer and the corresponding polymer were confirmed by ^1H NMR, FTIR and ^{13}C NMR. LC behavior of the polymer was investigated by differential scanning calorimetry (DSC), polarized light microscopy (POM). The electrochemical characterizations of PF ECS/rGO films were performed by cyclic voltammetry (CV), electrochemical impedance spectroscopy (EIS), typical amperometric response (IT) measurements. The ferrocenyl in polymer presented an excellent electrochemical behavior, and the modified electrode exhibited preferable electrocatalytic activity to the reduction of H_2O_2 . The work revealed that the developed electrochemical sensor detection of H_2O_2 with a higher sensitivity $117.142 \mu\text{A mM}^{-1} \text{cm}^{-2}$ and broader linear range between $1 \times 10^{-5} \text{ M}$ to $1.9 \times 10^{-4} \text{ M}$.

Key word: liquid crystalline polymer, reduced graphene oxide, sensor, hydrogen peroxide

Introduction

The fast, reliable and accurate detection of hydrogen peroxide (H_2O_2) has attracted considerable attentions because H_2O_2 is very common essential mediator in food, pharmaceutical, clinical and environmental analyses¹⁻⁴. At present, numerous methods have been developed to detect H_2O_2 , such as fluorometry, spectrometry, chemiluminescence, chromatography and electrochemical methods.⁵⁻¹¹ Among these methods, the electrochemical method has been extensively employed in the detection of H_2O_2 because of its simplicity, accurate, and fast response and economical efficiency for analysis. It is a great interest to reasonably fabricate an easy-to-made, sensitive, and cost-efficient sensor in the electrochemical method. Most of these methods are based on the immobilization of enzymes, such as horseradish peroxidase, cytochrome and myoglobin on the functionalized electrodes. Although the enzyme-based sensors have remarkable selectivity and high sensitivity for H_2O_2 detection, they usually suffer from the complicated enzyme

^aKey Laboratory of Special Functional Polymer Materials of Hunan Province, Key Laboratory of Advanced Functional Polymer Materials of Colleges and Universities of Hunan Province and Key Lab of Environment-friendly Chemistry and Application in Ministry of Education, College of Chemistry, Xiangtan University, Xiangtan 411105, Hunan Province, China.

* To whom the correspondence should be addressed.

E-mail: xhl20040731@163.com (HLX)

DOI: 10.1039/x0xx00000x

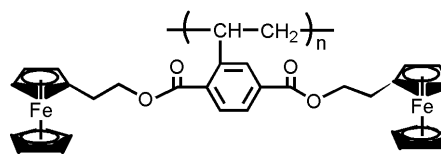
immobilization processes and effects of the experimental environment (pH, temperature, etc.).¹² At the same time, this kind of sensor lacks enough stability originating from the intrinsic nature of the enzymes. Therefore, numerous efforts have been devoted to the development of non-enzymatic electrochemical sensors.¹³⁻¹⁵

In the process of the developing the non-enzymatic electrochemical sensors, it is very important that how to increase the conductivity of the electrodes modified reasonably by the high conductive materials to improve the property of the electrochemical sensors. Graphene (Gr) is one of the most excellent candidates as the modifying materials for the electrodes because of its extra high surface area, rapid electron transport capability and thermal stability.¹⁶⁻¹⁸ Thus, in the past decades, numerous research has been devoted to graphene-based hybrid nanomaterials or nanocomposites for expending graphene performance.¹⁹ Furthermore, the graphene-based hybrid nanomaterial could be used to fabricate the novel mediate-free electrochemical biosensor.²⁰ It has been proved that Gr can efficiently promote electron transfer between the redox center and the electrode surface.²¹

Ferrocene (Fc) and its derivatives as the the most popular electrochemical active groups have been extensively used in non-enzymatic electrochemical sensors through chemically modified electrodes because of the redox reaction of Fc^+/Fc is completely reversible²². However, the adsorption of the ferrocene and its derivatives onto the the electrode surface is very poor. Thus, different methods have been developed to improve the adsorption of the ferrocenes on electrode surfaces to produce chemically-modified electrodes through incorporating ferrocenes into other system.²³⁻²⁵ Among these methods, the typical example is that the ferrocene covalently is bound to a flexible dendritic or polymeric backbone.²⁶ The resulting materials can be deposited onto surfaces or incorporated into carbon paste electrodes for H_2O_2 detection.

In this work, we designed and synthesized a rigid-chain liquid crystalline (LC) polymer (poly(2,5-bis ((2-ferrocenylethyl)oxy carbonyl)styrene) (PFECs)) using Fc unit to fabricate a novel nonenzymatic H_2O_2 sensor combining with the reduced graphene oxide (rGO). The chemical structure is shown in Scheme 1. It is noted that in this kind of polymer the side group with two ferrocenes every unit directly links to the main chain. Generally, in this kind of polymer the significantly high steric hindrance force the flexible backbone to form rather extended and stiff, and the whole molecular chain can be considered as a cylinder because the bulky side side groups located around the backbone are crowded.^{27,28} The typical example is mesogen-jacketed LC polymer (MJLCP).²⁹⁻³⁷ Thus, we expect the utilization efficiency of the ferrocenes would get improved because the extended and stiff main chain makes the ferrocenes more efficiently expose and contact each other. On the other hand, this kind of polymer would exhibit high electron transmission efficiency because of its every unit has two ferrocenes. At the same time, we have detailedly investigated the thermal stability, LC behavior of PFECs, and electrochemical behavior of the prepared modified electrode for detection of H_2O_2 . The result shows that the electrode modified by PFECs/rGO film present

desirable performance with good sensitivity for non-enzymatic H_2O_2 sensor applications.



Scheme 1. The chemical structure of PFECs.

Experimental

Materials

Tetrahydrofuran (THF) were dried, filtered and evaporated with vacuum distillation before use. 2,2'-azo-bis-isobutyronitrile (AIBN) was purified by recrystallization from ethanol. N,N-dimethylformamide (DMF) (Shanghai Chemical Reagents Co., A.R. grade), Dicyclohexylcarbodiimide (DCC), 4-dimethylaminopyridine (DMAP) (Shanghai Chemical Reagents Co.). Phosphate buffer solution (PBS) was prepared by mixing stock standard solution of Na_2HPO_4 and NaH_2PO_4 . Stock solutions of H_2O_2 were freshly diluted from 30% solution (Xilong Chemical Co. Ltd.). Graphite was obtained from Alfa Aesar. All other reagents were used as received from commercial sources.

Instruments and Measurements

1H NMR spectra were recorded on a Bruker ARX 400 MHz spectrometer with tetramethylsilane (TMS) as the internal standard and $CDCl_3$ as the solvent. GPC measurements were carried out at 35 °C on a Waters 1515 instrument equipped with three Waters μ -Styragel columns (10^3 , 10^4 , and 10^5 Å) in series, using THF as the eluent at a flow rate of 1.0 mL/min. The GPC data were calibrated with PS standards. Thermogravimetric analysis (TGA) was performed on a TA SDT 2960 instrument at a heating rate of 10 °C/min in air. Differential scanning calorimetry (DSC) experiments were carried out on a TA DSC Q100 calorimeter with a programmed heating and cooling procedure in nitrogen. The temperature and heat flow were calibrated with benzoic acid and indium. The samples were encapsulated in hermetically sealed aluminum pans with a typical sample weight of ~5 mg. The cooling and subsequent heating DSC experiments were carried out at a rate of 10 °C/min. LC texture of the polymers was examined under polarized optical microscope (POM, Leica DM-LM-P) coupled with a Mettler-Toledo hot stage (FP82HT). The films with a thickness of ~10 μm were casted from THF solution on glass slides and slowly dried at room temperature.

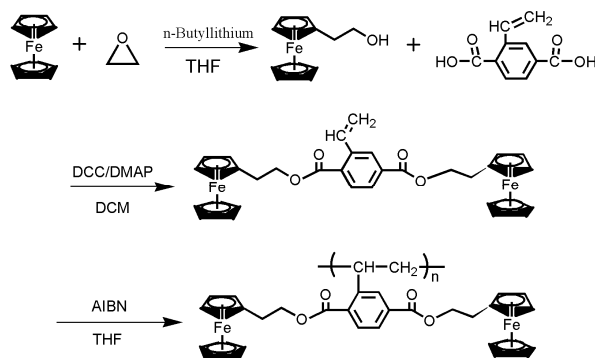
All electrochemical experiments were conducted on a CHI650D electrochemical workstation (Chenhua Instrument Company of Shanghai, China) in a conventional three-electrode system. The reference electrode was saturated calomel electrode (SCE), a platinum wire electrode was used as an auxiliary electrode and the working electrode was a modified GCE (3 mm diameter, Shanghai Chenhua, China). The pH measurements were carried out on PHS-

3C exact digital pH meter (Shanghai KangYi Co.Ltd.,China), which was calibrated with standard pH buffer solutions. Prior to each experiment, all solution was deoxygenated with high purity nitrogen and a nitrogen environment was then kept over the solution in the cell. All experiments were carried out at room temperature.

Experimental section

Synthesis

The synthetic route of PEECS and the corresponding monomer are shown in Scheme 2. And the detail information about the synthesis and character of the intermediate and monomers are presented as following.



Scheme 2. Synthetic route of the monomer and the corresponding polymer.

Synthesis of 2-Ferrocenylethyl Alcohol

2-Ferrocenylethyl Alcohol was synthesized according to previously reported literature.³⁸ Yield: 39.4% ¹H NMR (CDCl₃) δ (ppm): 4.18 (br s, 9H, Cp), 3.72 (m, 2H, OCH₂), 2.59 (t, J = 6.5 Hz, 2H, OCH₂CH₂).

Synthesis of 2-Vinyl p-Biphthalic Acid

Vinyl p-biphthalic acid was prepared using the procedure described in the previous literature.³⁹ ¹H NMR (DMSO-*d*₆) δ (ppm): 8.24 (s, 1H, Ar-H), 7.92 (d, 2H, Ar-H), 6.67 (d, 2H, =CH-), 5.75 (d, 1H, =CH₂), 5.42 (d, 1H, =CH₂)

Synthesis of the Monomer FECS

2-Ferrocenylethyl Alcohol (2.3 g, 10 mmol), Vinyl p-biphthalic acid (768 mg, 4 mmol), DCC (3.3 g, 16 mmol) and DMAP (0.097 mg, 0.8 mmol) were dissolved in DMF (30 mL). After stirring overnight at room temperature, the reaction mixture was filtered and the filtrate was reduced pressure distillation. The crude product was purified by column chromatography (SiO₂, n-hexane/diethyl ether=3/8) to afford the product as a orange solid (0.54 g) with a yield of 34.9%. ¹H NMR (CDCl₃) δ (ppm): 8.24 (s, 1H, Ar-H), 7.94 (d, 2H, Ar-H), 5.78 (d, 2H, =CH-), 5.44 (d, 1H, =CH₂), 5.41 (d, 1H, =CH₂), 4.48(m, 2H, OCH₂), 4.15 (br s, 9H, Cp), 2.81 (t, J = 6.5 Hz, 2H, OCH₂CH₂). IR (KBr, cm⁻¹): ν 3090 (w), 2960 (w), 2845 (w), 1561 (w), 1482 (w), 1452 (w), 1295 (m), 1239 (s), 1186 (m), 1107 (s), 1057 (m), 994 (m), 921 (m), 821 (m), 797 (s), 759 (s), 718 (m). ¹³C

NMR (CDCl₃) δ (ppm): 29.12 (-OCH₂CH₂), 66.05-75.4 (Cp-C), 68.7 (-OCH₂CH₂), 117.8(=CH₂), 128.15 (aromatic C ortho to C-CH=CH₂), 128.36 (-C-CH=CH₂), 130.45 (aromatic C ortho to C-C=O), 132.51 (aromatic C ortho to C-C=O), 133.33 (C-C=O), 134.95 (-CH=CH₂), 139.56 (C-C=O), 165.54 (C=O), 166.74 (C=O).

Synthesis of the Polymer PFECS

The synthetic route of PFECS is described in Scheme 2. The polymer was obtained by conventional radical polymerization. FECS (0.7 g, 1.8 mmol), 1 mg/mL THF solution of AIBN (1.59 mL) and THF (1.39 g) were transferred into a polymerization tube. After three freeze-pump-thaw cycles, the tube was sealed off under vacuum. Polymerization was carried out at 65°C for 12 h. Then the tube was then opened, and the reaction mixture was diluted with THF, and then reprecipitated in petroleum ether. The polymer was dried to a constant weight. Yield: 72%.

Preparation of the PFECS/ rGO modified electrode

The graphite oxide (GO) powder was prepared from graphite powder via a modified Hummers' method. The surface of electrode was polished successively with 0.3, 0.1 and 0.05 μm alumina slurry and then cleaned under ultra sonication in ethanol and water, respectively. Then, 5 μL the GO solution was casted on the surface of glassy carbon electrode (GCE) and allowed to dry at ambient temperature. Cyclic voltammograms (CV) was used to reduce GO at a potential range from 0 V to -1.4 V in 0.02 M pH=5.6 phosphate buffer solution with N₂-saturated. In this work, 40 cycles were adopted for the reductive adsorption of GO on the electrode. While the tiled graphene modified electrode was obtained. The graphene modified electrodes were then dried under ambient temperature. 5.0 mg PFECS were dispersed in 5.0 mL DCM. Then 5 μL of 5.0 mg mL⁻¹ PFECS solution and equivalent volume of the resulting mixture were dropped onto the rGO modified electrode surface successively and dried in room temperature. The modified electrodes were stored at 4°C in a refrigerator.

Results and Discussion

Synthesis and Characterization of PFECS

The objective polymer was readily obtained by radical polymerization method because the monomer has vinyl substituent. Figure 1 depicts the ¹H NMR spectra of the monomer and the polymer, wherein the assignments of resonance peaks are included. The characteristic resonance peaks of the vinyl substituent of corresponding monomer FECS at chemical shifts of 5.78, 5.74, 5.44, and 5.41 ppm (denoted as e and f, respectively) disappeared completely after polymerization. Moreover, the chemical shifts of PFECS became quite broad compared to the monomer FECS, which was consistent with the polymer structure expected. Generally, the formation of film and was strongly depended on the molecular weight (MW), and the kind of LC polymer presented LC behavior only its MW exceeded a critical value. Thus, we furthermore used GPC to characterize the the MW and polymer polydispersity index (PDI). The result showed its MW was 6.0 × 10⁴ and the PDI was 1.83. According to the previous

results, the present MW was big enough to prepare film and present LC behavior.

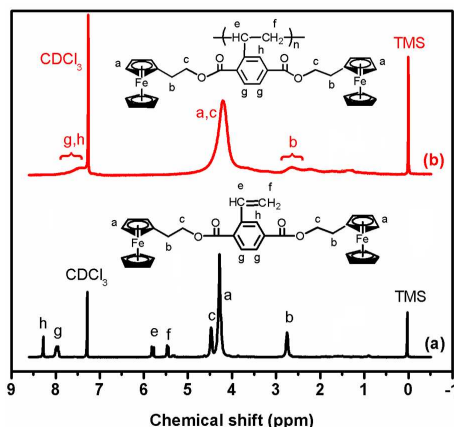


Figure 1. ^1H NMR spectra of FECS and the PF ECS

Thermal and LC properties of the PF ECS

In present system, the annealing process was beneficial to the development of LC phase and film formation, which was important for the chemical or electrochemical property. Thus, we firstly investigated the thermal stability of PF ECS. TGA experimental results revealed that the thermal decomposition temperature of the PF ECS was above $340\text{ }^\circ\text{C}$, indicating that this kind of polymer had good thermal stabilities.

To investigate the liquid-crystalline behavior of PF ECS, the combined techniques of DSC and POM were employed to use. The sample was completely dried under vacuum before performing the DSC analysis. To eliminate the effect of thermal history, the sample was heated from room temperature to $150\text{ }^\circ\text{C}$ with a rate of $10\text{ }^\circ\text{C}/\text{min}$, kept at $150\text{ }^\circ\text{C}$ for 5 min and then cooled to $0\text{ }^\circ\text{C}$ at a rate of $10\text{ }^\circ\text{C}/\text{min}$. Figure 2(a) describes of DSC heating traces of the PF ECS recorded at a rate of $10\text{ }^\circ\text{C}/\text{min}$ after erasing the sample's thermal history. The DSC measurements showed only a glass transition step at about $93\text{ }^\circ\text{C}$ but no endothermic peak correlative to any melting of crystals. This result was the same to the traditional MJLCPs⁴⁰.

Before the POM experiment, the sample was casted from THF solution and slowly dried at room temperature. The POM micrographs of the polymer were recorded during the first cooling process. The experimental phenomenon showed the samples presented birefringence under different temperature. Even cooling to room temperature, the birefringence still remained. All results revealed the sample formed stable LC phase under different temperature.⁴¹ Obviously, the kind of polymer didn't include LC mesogens. Thus, the LC phenomenon could be explained by the chain conformation, that was, the bulky side group constituted of two ferrocenes and one benzene located around the backbone were crowded, and the significantly high steric hindrance forced the flexible polyolefin backbone to become rather extended and stiff, and the whole molecular chain would be considered as a molecule, furthermore, the LC molecule self assembly into LC phase, which was similar to the previous results reported in the literature.⁴²

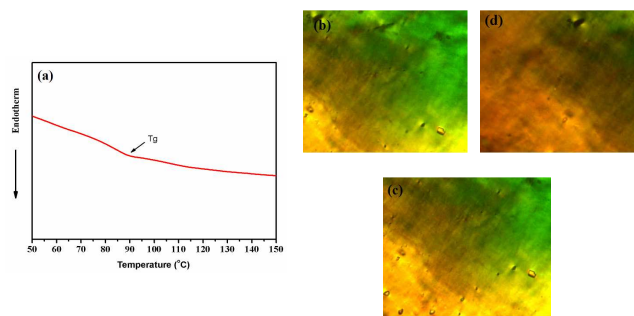


Figure 2. (a) DSC curves of the polymer PF ECS, (b), (c), (d) POM micrographs of PF ECS (magnification $200\times$).

Direct electrochemical of PF ECS/rGO modified electrode

Figure 3 shows the CV of different electrodes modified in deaerated 0.2 M PBS (pH 7.0). For PF ECS/GCE, a pair of small redox peaks consisted of an anodic peak at 0.526 V and a cathodic peak at 0.402 V was observed. Compared with electrode modified by PF ECS, the peak currents of electrode modified by PF ECS/rGO increased obviously, and a pair of well-defined redox peaks was observed. The anodic peak potential (E_{pa}) and cathodic peak potential (E_{pc}) were located at 0.535 V and 0.462 V , respectively. The formal potential (defined as the midpoint of reduction and oxidation potentials), E^0 was 0.486 V for PF ECS. The peak potential separation (E_p , defined as $E_p = E_{pa} - E_{pc}$) was calculated as 73 mV . All the above results revealed that the direct electron transfer between PF ECS and electrode was greatly enhanced.

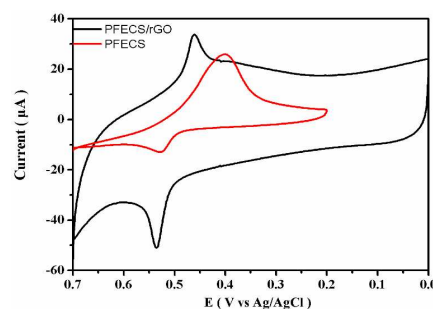


Figure 3. The CV of different materials modified electrodes in 0.2 M PBS at a scan rate of 100 mV s^{-1} .

The film conductivity in the presence of rGO was studied by electrochemical impedance spectroscopy (EIS). Figure 4 describes the electrochemical impedance spectra of different modified electrode. The electron transfer resistance (R_{et}) at the electrode surface could be used to describe the interface properties of the electrode, which was equal to the semicircle diameter of electrochemical impedance spectra. For electrochemical impedance spectrum of GCE, the semicircle domain was very small ($R_{et} = 1338\ \Omega$), which indicated very low electron transfer resistance to the redox-probe dissolved in the electrolyte solution. However, the R_{et} ($2681\ \Omega$) of the PF ECS modified electrode was much larger than that

of the GCE. It implied that PF ECS film on the electrode surface could inhibit the electron transfer of the redox-probe of $[\text{Fe}(\text{CN})_6]^{3-}/^{4-}$ to the electrode surface to a certain degree. After added rGO, the Ret of PF ECS/rGO modified electrode decreased to about 302Ω , indicating that rGO had good conductivity and the PF ECS/rGO film could make the electron transfer more easily.

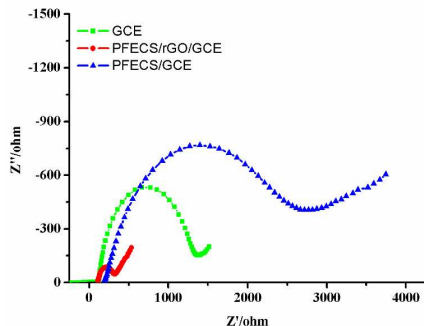


Figure 4. Electrochemical impedance spectra of different modified electrode at the open circuit potential in 0.2 M PBS, pH=7.0, containing 5 mM $\text{K}_3\text{Fe}(\text{CN})_6$ and 5 mM $\text{K}_4\text{Fe}(\text{CN})_6$.

The CVs of PF ECS/rGO modified electrode with different scan rates were measured as shown in Figure 5. A series of well-defined redox peaks shape was observed with different scan rates in the range of $0.05\text{--}0.15 \text{ V s}^{-1}$, which showed almost equal heights of reduction and oxidation peaks at the same scan rate. As seen in Figure 5(b), the anodic and cathodic peak current for PF ECS/rGO modified electrode exhibits a linear relationship with the scan rate, indicating a typical surface-controlled electrode process.

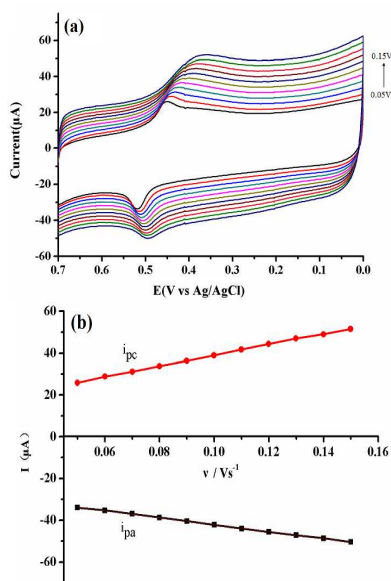
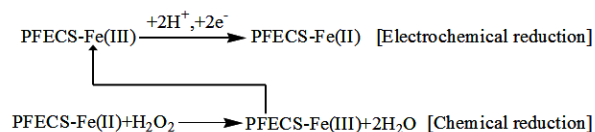


Figure 5. (a) CVs of PF ECS/rGO/GCE in PBS (pH 7.0) at different scan rates. (b) plot of the peak current i against the scan rate v .

Electrochemical response to H_2O_2 at the PF ECS/rGO modified electrode

Electroanalytical method of the PF ECS/rGO film electrode could be applied in the analysis of H_2O_2 . Figure 6 shows the cyclic voltammograms of the PF ECS/rGO modified electrode in 0.2 M pH 7.0 PBS in the absence and presence of different amount of H_2O_2 at 0.1 V s^{-1} . When H_2O_2 was added into the blank buffer, a dramatic change in the cyclic voltammogram occurred with an increase in cathodic current. The catalytic reduction occurred at potential of 0.4 V at the modified electrode. A significant improvement of the cathodic current reflected the high electrocatalytic activity of the PF ECS/rGO modified electrode. The mechanism of electrocatalytic reduction of H_2O_2 at PF ECS/rGO film electrode is given in Scheme 3. The ferrocenyl in PF ECS which was in the oxidised form at the electrode surface gets reduced at the applied potential. This reduced form of the mediator in turn reduces H_2O_2 in solution and gets oxidised. The regenerated oxidised form of PF ECS at the surface of the electrode again got reduced producing the reduction current at the same time. The process of analyte reduction and catalyst regeneration proceeds in a cyclic manner enhancing the reduction current of the mediator.⁴³



Scheme 3. Mechanism of H_2O_2 reduction with PF ECS /rGO.

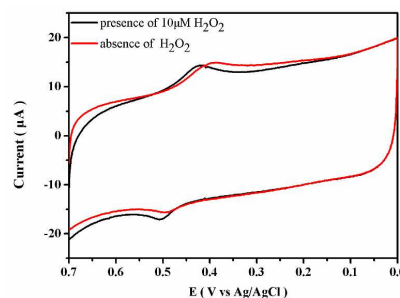


Figure 6. CVs of PF ECS/rGO in 0.2 M PBS (pH 7.0) in the presence and absence of H_2O_2 .

The PF ECS/rGO modified electrode could also be used as an amperometric sensor for the detection of H_2O_2 . Typical current-time (i - t) curves for the modified electrodes (PF ECS/rGO) with successive addition of H_2O_2 at a working potential of 0.44 V (V vs. Ag/AgCl) are presented in Figure 7. When H_2O_2 solution was continuously injected into the PBS solution, the current was increased and then reached to steady with a response time lower than 3 s, indicating a fast response. This phenomenon was mainly due to the existence of Fc and the well-conductive properties of the PF ECS. At the same time, a shift of peak potential could also be observed in Figure 6, where the explanation was expecting for further research. Figure 7 shows the change in the response current

with the concentration of H_2O_2 . The reduction currents were proportional to the concentration of H_2O_2 ranging from 1.0×10^{-5} to 1.9×10^{-4} M, with a regression equation of $I_p (\mu\text{A}) = -0.0082C - 0.06824 (\mu\text{M})$ ($R^2 = 0.999$). The sensitivity of the PF ECS/rGO sensor was calculated as $117.142 \mu\text{A mM}^{-1} \text{cm}^{-2}$ by dividing the slope of the linear regression equation by the electrode surface area.

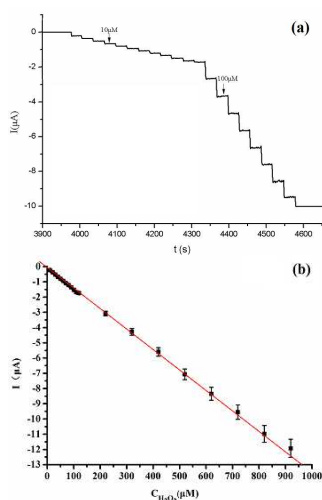


Figure 7. (a) Amperometric response of the H_2O_2 sensor to successive addition of different concentration of H_2O_2 in PBS solution (pH = 7.0) at the working potential of 0.44 V. (b) plot of electrocatalytic peak current vs. concentration of H_2O_2 .

A comparison of this PF ECS/rGO/GCE with other H_2O_2 sensors reported in the literature are shown in Table 1 in terms of linear detection range (LDR), limit of detection (LOD) and sensitivity. The analytical performances for PF ECS/rGO/GCE are comparable and better than those obtained on other electrodes reported recently. Therefore, the PF ECS/rGO/GCE can be used as a non-enzyme platform for the effective detection of H_2O_2 with low LOD and high sensitivity. It indicates in Table 1 that the limit of detection of the sensor is relative lower than previous reports. Meanwhile, in order to test the repeatability, reproducibility and re-usability of the sensor, the relative standard deviation (RSD) and the response current depended on the time are shown in Figure 1 and Figure 2 in the supporting information, indicating the PF ECS/rGO/GCE possessed acceptable reproducibility and stability. Moreover, the possible interferences from some co-existing electroactive compounds were assessed in order to investigate the selectivity of the developed non-enzymatic sensor as show in Figure 3 of the supporting information. It reveals that the proposed non-enzymatic electrode can be employed in the selective detection of H_2O_2 in the presence of these common physiological materials.

Obviously, the result indicated that this novel composites PF ECS/rGO presented excellent electrochemical properties, which could be used for the detection of H_2O_2 . Compared to the other polymer, the whole molecular chain of the polymer PF ECS would be considered as a cylinder because the significantly high steric

hindrance force the flexible backbone to become rather extended and stiff. At the same time, the side group with two ferrocenes every unit which was helpful to high electron transmission efficiency was located around the backbone. We speculated the stiff main chain and high density electronic sites may make the ferrocenes more efficiently expose and contact each other, which may be a new strategy for molecular design using sensor's material. According to this idea, the relative optimization results will report in the following work.

Table 1. Comparison of various H_2O_2 sensors.

Electrode	LDR(μM)	LOD(μM)	Sensitivity($\mu\text{A mM}^{-1} \text{cm}^{-2}$)	Reference
Pt/PPy/GC/GCE	100–800	1.2	80	[44]
GN-AuNPs/GCE	20–280	60	-	[45]
PPy/Mn NWs	5–90	2.12	3.79	[46]
Graphene/PB/GCE	20–200	1.9	196.6	[47]
Grass-like CuO with calcination	10–300	4.3	119.35	[48]
PF ECS/rGO/GCE	10–190	1.253	117.142	This work

Conclusions

The monomers 2,5-bis [(2-ferrocenylethyl)oxy carbonyl]styrene were successfully synthesized and the corresponding polymer was easily obtained via radical polymerization. The chemical structure of the polymer was confirmed by various characterization techniques. The polymer showed good thermostability and birefringent melts. Furthermore, based on a new PF ECS/rGO composite film, a novel amperometric H_2O_2 biosensor was designed. The rGO have improved the conductivity and mechanical properties of the PF ECS. Combining the advantages of PF ECS and rGO the modified electrode showed good analytical performance, such as high sensitivity and storage stability. Hence, it provides a promising application for developing nonenzymatic sensor with transition metal and rigid chain LC polymers materials.

Acknowledgments

This research is financially supported by the National Nature Science Foundation of China (21374092), the project of Hunan Provincial Education Department (YB2013B032), Innovation Platform Open Foundation of University of Hunan Province (14K093) and Beijing National Laboratory for Molecular Sciences (BNLMS).

Notes and references

- 1 N. Akhtar, A. Md. Khairy and A. El-Saida, *Sensors and Actuators B: Chemical*, 2015, **207**, 158.
- 2 Y. A. Chang., Kai Z., Kim W.J. and C.H. Chung, *Sensors and Actuators B: Chemical*, 2015, **213**, 329.

- 3 Y.C Li., Y.Y.Zhang, Y.M Zhong, and Li. S.X., *Applied Surface Science*, 2015, **347**, 428.
- 4 Q.W Liu, T. Zhang , L.L.Yu , N. Q.Jia. and D.P Yang. , *Analyst*, 2013, **138**, 5559.
- 5 G. B. Xu and S. J. Dong , *Electroanalysis*, 1999, **11**, 1180.
- 6 N.Masuoka , M.Wakimoto, T.Ubuka and T.Nakano, *Clinica Chimica Acta*, 1996, **254**, 101.
- 7 F.J. Pérez and S. Rubio, *Plant Growth Regulation*, 2006, **48**, 89.
- 8 Y. zong and Li A.T, *Analytica chimica acta*, 1998, **359**, 149.
- 9 S.L. Rasmus, K. Peterand K. Uwe, *Analytical Chemistry*, 2003, **75**, 731.
- 10 Li F. , Chen W. , Tang C.F and Zhang S. , *Talanta*, 2009, **77**, 1304.
- 11 L. Xingping, X. Xianping and L. Zhuang, *Analytical Methods*, 2014, **6**, 235.
- 12 Li X.Y, Liu Y.X. , Zheng. L.C. , Dong. M.J. , Xue. Z.H. , Lu X.Q and Liu X.H , *Electrochimica Acta*, 2013, **113**, 170.
- 13 H. Sijing , C. Zuanguang, Y. Yanyan and S. Lijuan, *RSC Advances*, 2014, **4**, 45185.
- 14 James D. G., Ajay S. Karakoti, Talgat Inerbaev, Shail Sanghavi, P. Nachimuthu, V. Shutthanandan, S. Seal and S. Thevuthasan, *Journal of Materials Chemistry B*, 2013, **1**, 3443.
- 15 L. Hua-Jun, Y. Dong-Wei and L. Hui-Hong, *Analytical Methods*, 2012, **4**, 1421.
- 16 Y. Suling, L. Gang, W. Guifang, Z. Junhong, H. Meifang and Q. Lingbo, *Sensors and Actuators B: Chemical*, 2015, **208**, 593.
- 17 L. Farnaz, S. Zohreh, M. Pooria, A. Yatimah and M. Ninie S.A. , *Sensors and Actuators B: Chemical*, 2015, **208**, 389.
- 18 L. Panpan , L. Jiawei , L. Xiuhui , L. Ming and L. Xiaoquan , *Journal of Electroanalytical Chemistry*, 2015, **751**, 1.
- 19 Lee. C, Wei. XD, Kysar. JW and Hone. J, *Science*, 2008, **321**, 385.
- 20 P. Pengfei , Y. Zhongming , X. Shixiu , X. Jinling , Z. Yanli and G. Yuntao , *Journal of Electroanalytical Chemistry*, 2014, **727**, 27.
- 21 Y. Yiping , K. Tao , Y. Xiaofang and W. Yukun , *Talanta*, 2012, **89**, 417.
- 22 Z. Guang-Chao, X. Miao-Qing and Z. Qiang, *Electrochemistry Communications*, 2008, **10**, 1924.
- 23 G. Tanushree , S. Priyabrata and T. Anthony P.F. , *Bioelectrochemistry*, 2015, **102**, 1.
- 24 L. Ting and Y. Minghui , *Sensors and Actuators B: Chemical*, 2011, **158**, 361.
- 25 L. Yizhong , J. Yuanyuan , W. Haibin and C. Wei , *Electrochimica Acta*, 2015, **156**, 267.
- 26 R. K. Nagarale, L. Jong Myung and S. Woonup, *Electrochimica Acta*, 2009, **54**, 6508.
- 27 W. Junji, S. Nobuhiro, N. Tokihiro and S. Masato, *Macromolecules*, 1996, **29**, 4816.
- 28 R. Brad M., W. Christopher J., W. Daniela A., P. Mihai, I. Mohammad R. and P. Virgil, *Chemical Reviews*, 2009, **109**, 6275.
- 29 Q. F Zhou., A.M Li. and X. D Feng., *Macromolecules*, 1987, **20**, 233.
- 30 L. Weng, J.J Yan, H.L Xie, G.Q Zhong, S. Q Zhu, H.L Zhang and E.Q Chen, *Journal of Polymer Science Part A-Polymer Chemistry*, 2013, **51** , 1912.
- 31 G.H. Wen, B. Zhang, H.L Xie, X Liu, G.Q Zhong, H.L Zhang and E.Q Chen, *Macromolecules*, 2013, **46** , 5249.
- 32 H.L. Xie, S.J Wang., G.Q.Zhong, Y.X Liu, H.L Zhang and E.Q Chen, *Macromolecules*, 2011, **44**, 7600.
- 33 H.L. Xie, C.K. Jie, Z.Q. Yu, X.B. Liu, H.L. Zhang, ZH.Shen, E.Q. Chen and Q.F. Zhou, *Journal of the American Chemical Society*, 2010, **132**, 8071.
- 34 H.L. Xie, Y.X Liu., G. Q. Zhong, H.L. Zhang, E.Q. Chen and Q.F. Zhou , *Macromolecules*, 2009, **42**, 8774.
- 35 D. We, B. i Annie, A. Pierre-antoine, P. Keller, X. G Wang and M.H Li, *Chinese Journal of Polymer Science* , 2012, **30**, 258.
- 36 Q. Bi-wei, C. Feng, S. Yong-gang, L. Yu and Q Zhen., *Chinese Journal of Polymer Science*, 2015, **33**, 95.
- 37 X B Liu., Y. F Zhu. , H Fan and E. Q Chen, *Chinese Journal of Polymer Science*, 2013, **31**, 946.
- 38 Y. Yali, X. Zuowei and C Wu. *Macromolecules*, 2002, **35**, 3426.
- 39 D. Zhang., L. Yuxiang , X H Wan and Q. F Zhou, *Macromolecules*, 1999, **32**, 4494.
- 40 D. Zhang., L. Yuxiang , X H Wan and Q. F Zhou, *Macromolecules*, 1999, **32**, 5183.
- 41 S.P. Hendry, M.F. Cardosi, A.P.F. Turner and E.W. Neuse, *Analytica Chimica Acta*, 1993, **281**, 453.
- 42 A. Wael A., L. Wang, A. Abid M., Y. Haojie, Z. Lei , L. Chao and W. Yang , *Polymers for Advanced Technologies*, 2013, **24**, 181.
- 43 G. A. M. Pilar, L. José, C. Isabel, A. Beatriz , G. Blanca, C. Carmen M. and Z. Jinbiao, *Sensors and Actuators B: Chemical*, 2004, **101**, 143.
- 44 X. Bian, X. Lu, E. Jin, L. Kong, W. Zhang and C. Wang, *Talanta* 2010, **81**, 813.
- 45 J. Hu, F. Li, K. Wang, D. Han, Q. Zhang, J. Yuan and L. Niu, *Talanta*, 2012, **93**, 345.
- 46 M.R. Mahmoudian, Y. Alias, W.J. Basirun, A.M. Golsheikh and F. Jamali-Sheini, *Materials Chemistry and Physics*, 2013, **141**, 298.
- 47 E. Jin, X.F. Lu, L.L. Cui, D.M. Chao and C. Wang, *Electrochimica Acta*, 2010, **55**, 7230.
- 48 P. Gao, G. Yuxuan, P. M. Nathan and L.Dawei, *Electrochimica Acta*, 2015, **173**, 31.

Graphic Abstract

Design and Preparation of Non-enzymatic Hydrogen Peroxide Sensor based on a Novel Rigid Chain Liquid Crystalline Polymer/Reduced Graphene Oxide Composite

Ya-qi Yang, He-lou Xie*, Jun Tang, Shuai Tang, Jie Yi*, Hai-liang Zhang*

Key Laboratory of Special Functional Polymer Materials of Hunan Province, Key Laboratory of Advanced Functional Polymer Materials of Colleges and Universities of Hunan Province and Key Lab of Environment-friendly Chemistry and Application in Ministry of Education, College of Chemistry, Xiangtan University, Xiangtan 411105, Hunan Province, China

A novel non-enzymatic hydrogen peroxide (H_2O_2) sensor was developed using rigid chain liquid crystalline (LC) polymer with ferrocenyl as the side group and reduced graphene oxide (rGO) composite.

